Theoretical Performances Analysis of the Blind Multiuser Detection based on Fluctuations of Correlation Estimators in Multirate CDMA Transmissions

Crépin Nsiala-Nzéza, Roland Gautier, Gilles Burel

MTA Review, Vol. XVIII, No. 2, pp. 119-140, Jun. 2008 (ISSN 1843-3391)

THEORETICAL PERFORMANCES ANALYSIS OF THE BLIND MULTIUSER DETECTION BASED ON FLUCTUATIONS OF CORRELATION ESTIMATORS IN MULTIRATE CDMA TRANSMISSIONS

C. Nsiala Nzéza[1], R. Gautier, and G. Burel
LEST/TST UMR-CNRS 6165, Université de Bretagne Occidentale, Brest, France
roland.gautier@univ-brest.fr
http://www.univ-brest.fr/lest/tst

***Abstract* - This paper deals with the problem of blind multiuser detection in multirate direct-sequence code division multiple access (DS-CDMA). Direct-Sequence Spread Spectrum (DS-SS) signals are well-known for their low probability of interception: their statistics are similar to that of a noise; furthermore, they are usually transmitted below the noise level. We tackle here the theoretical performances, in terms of probability of detection and false alarm of the method based on the fluctuations of autocorrelation estimators. Numerical results will illustrate the efficiency of the method.**

1. Introduction

One of the salient features of CDMA-based third-generation (3G) wireless systems is the capability to support transmission of diverse data such as voice, low-resolution video, compressed audio... Since these heterogeneous services produce digital information streams with different data rates, their implementation requires the use of multirate CDMA systems where each user may transmit his data at one among a set of available data rates. An easy way to view the multirate CDMA transmission is to consider the variable spreading length (VSL) technique where all users employ sequences with the same chip period. Moreover, each data rate is tied to the length of the spreading code of each user.

Many blind approaches have been devised to either improve the performance of a CDMA receiver in a multirate multiuser context or reduce its complexity. Some prior knowledge of user parameters, e.g. the signature waveform [1], the processing gain, the code of a group of active users [2], the chip rate [2], [3] is always assumed, but its nature depends on the technique employed.

Thus, we recently proposed a blind multiuser detection scheme requiring no prior knowledge about the transmitter [4]. Therefore, its performances have to be analyzed in order to evidence its efficiency prior to any further implementation in operational systems, which is of great interest for both military and civil applications.

The remainder of the paper is organized as follows. Section 2 introduces the signal model and assumptions made. Section 3 briefly describes the blind-detection approach, while Section 4 highlights its performances in terms of probability of detection and false alarm. Finally, numerical results are detailed in Section 5, and conclusions are drawn in Section 6.

---

[1] *Crépin Nsiala Nzéza is now with the Integrated Circuits Design Group, IEMN/ISEN UMR-CNRS 8520, Lille, France, crepin.nsiala@isen.fr*

2. Signal modeling and assumptions

Let us consider the general case of asynchronous DS-CDMA system where each user can transmit at one out of S available data rates $R_0 < R_1 < \cdots < R_{S-1}$. By denoting N_u^i the number of active users transmitting at R_i and N_u the total number of users such that $\sum_{i=0}^{S-1} N_u^i = N_u$, the complex equivalent model of the received signal can be expressed as

$$y(t) = \sum_{i=0}^{S-1} \sum_{n=0}^{N_u^i - 1} \sum_{k=-\infty}^{+\infty} a_{n,i}(k) h_{n,i}(t - kT_{s_i} - T_{d_{n,i}}) + b(t), \tag{1}$$

where $h_{n,i}(t) = \sum_{k=0}^{L_i - 1} c_{n,i}(k) p_i(t - kT_c)$. In (1), the subscript $(\cdot)_{n,i}$ refers to the n^{th} user transmitting at R_i, denoted throughout this report as the $(n,i)^{th}$ user. Accordingly

- $a_{n,i}(k)$ are the baseband symbols of variance $\sigma^2_{a_{n,i}}$ for the $(n,i)^{th}$ user, whereas $p_i(t)$ is the convolution of the transmission filter, channel filter (which takes into account channel echoes, fading, multipaths and jammers) and receiver filter for each rate.
- $h_{n,i}(t)$ is a virtual filter corresponding to the convolution of all filters of the transmission chain with the spreading sequence $\{c_{n,i}(k)\}_{k=0 \cdots L_i - 1}$, where L_i is the spreading factor for the $(n,i)^{th}$ user.
- Because of the VSL technique, the symbol period T_{s_i} for the users transmitting at the rate R_i is tied to the common chip period T_c: $T_{s_i} = L_i T_c$, and $s_{n,i}$ stands for the $(n,i)^{th}$ signal.
- $T_{d_{n,i}}$ is the corresponding transmission delay for the $(n,i)^{th}$ user; it is assumed to satisfy $0 \le T_{d_{n,i}} < T_{s_i}$ and to remain constant during the observation.
- $b(t)$ is a centered additive white Gaussian noise (AWGN) of variance σ_b^2.
- Signals are assumed to be independent, centered, noise-unaffected and received with the same power $\sigma^2_{s_{n,i}} = \sigma^2_{s_{0,0}}$, for all (n,i).
- The signal-to-noise ratio (SNR) in dB) at the detector input is negative (signal hidden in the noise).

By denoting $s(t)$ the global noise-unaffected received signal, (1) can be rewritten as

$$y(t) = s(t) + b(t) = \sum_{i=0}^{S-1} \sum_{n=0}^{N_u^i - 1} s_{n,i}(t - T_{d_{n,i}}) + b(t). \tag{2}$$

3. Blind detection approach

As explained in [5], the analysis of the autocorrelation fluctuations estimators allows to achieve a blind multiuser detection. Successive investigations of the contributions of noise and signal through the analysis of the second-order moment of the autocorrelation estimator allowed its description, as hereinafter briefly reported.

The received signal is first divided into M temporal windows, each of them of duration T_F. Then, within each window m, an estimation of its autocorrelation is computed as

$$\hat{R}_{yy}^{m}(\tau) = \frac{1}{T_F}\int_0^{T_F} y_m(t) y_m^*(t-\tau)dt, \tag{3}$$

where $y_m(t)$ is the signal sample over the m^{th} window. Hence, the second-order moment of the estimated autocorrelation $\hat{R}_{yy}(\tau)$ using M windows can be expressed as

$$\Phi(\tau) = \hat{E}\left\{ | \hat{R}_{yy}(\tau) |^2 \right\} = \frac{1}{M}\sum_{m=0}^{M-1} | \hat{R}_{yy}^{m}(\tau) |^2, \tag{4}$$

where $\hat{E}(\cdot)$ is the estimated expectation of $(\cdot)$. Hence, $\Phi(\tau)$ is a measure of the fluctuations of $\hat{R}_{yy}(\tau)$. It is composed of fluctuations $\Phi_s(\tau)$ and $\Phi_b(\tau)$ due to noise-unaffected signals and the noise, respectively. Moreover, since fluctuations are computed from many randomly-selected windows, they do not depend on the signals relative delays $T_{d_{n,i}}$.

First, only the fluctuations due to the additive noise are uniformly distributed over all values of τ. Depending on the spreading sequence properties, the Multiple Access Interference (MAI) noise generates rather null, or very low incoherent fluctuations. Since the noise is random, the fluctuations of the autocorrelation estimator, denoted $\Phi_b(\tau)$, are also random. Assuming a receiver filter with a flat frequency response in $[-W/2, +W/2]$ and zero outside, they can be characterized by their mean m_{Φ_b} and standard deviation σ_{Φ_b} as follows [5]:

$$m_{\Phi_b} = \frac{\sigma_b^4}{WT_F} \text{ (a)} \qquad \sigma_{\Phi_b} = \sqrt{\frac{2}{M}}\frac{\sigma_b^4}{WT_F} \text{ (b).} \tag{5}$$

Second, by only considering the independent, centered and noise-unaffected signal, it was shown that, on average, high amplitudes of the fluctuations $\Phi_s(\tau)$ of the autocorrelation estimators occur for τ multiple of T_{s_i}, $i = 0, \cdots, S-1$. Let us set as $\Phi_i(\tau)$, the fluctuations due to the N_u^i signals transmitting at R_i

$$\Phi_i(\tau) = m_{\Phi_i} \cdot pgn_{T_{s_i}}(\tau), \tag{6}$$

where $pgn_{T_{s_i}}(\tau) = \sum_{k=-\infty}^{+\infty} \delta(\tau - kT_{s_i})$, $\delta(\tau) = 1$ for $\tau = 0$, and $\delta(\tau) = 0$ if $\tau \neq 0$. Thus, the fluctuations due to the global noise-unaffected signal are:

$$\Phi_s(\tau) = \sum_{i=0}^{S-1} \Phi_i(\tau) = \sum_{i=0}^{S-1} m_{\Phi_i} \cdot pgn_{T_{s_i}}(\tau). \tag{7}$$

Since signals are assumed to be received with the same power (e.g., $\sigma_{s_{0,0}}^2$) and $T_{s_i} = L_i T_c$, the fluctuations $\Phi_i(\tau)$ average amplitude m_{Φ_i} can be written as

$$m_{\Phi_i} = N_u^i \frac{T_{s_i}}{T_F}\sigma_{s_{0,0}}^4 = N_u^i \frac{L_i T_c}{T_F}\sigma_{s_{0,0}}^4 \tag{8}$$

Equation (8) shows an increase in the average fluctuations amplitude concomitant with that of the number of users. It also indicates that the average fluctuations amplitude is tied to the sequence lengths.

Let us at last compute the standard deviation, σ_{Φ_i}, of Φ_i within each group i. The

hypothesis of noise-unaffected and independent signals leads to

$$\Phi_i(\tau) = \sum_{n=0}^{N_u^i - 1} \Phi_{s_{n,i}}(\tau). \tag{9}$$

As detailed in [6][Chap. 3,pp. 38-39], since the fluctuations are computed from many independent randomly-selected windows, $\Phi_{s_{n,i}}(\tau)$ is similar to a Gaussian distribution. Consequently the variance $\sigma^2_{\Phi_i}$ is written as

$$\sigma^2_{\Phi_i} = \sum_{n=0}^{N_u^i - 1} \sigma^2_{\Phi_{s_{n,i}}}, \tag{10}$$

where $\sigma^2_{\Phi_{s_{n,i}}}$ stands for the variance of fluctuations due to the $(n,i)^{th}$ signal. Then, from (10), the standard deviation σ_{Φ_i} can be expressed as

$$\sigma_{\Phi_i} = \sqrt{\frac{2}{M}} \frac{N_u^i L_i T_c}{T_F} \sigma^4_{s_{0,0}}. \tag{11}$$

Equation (11) evidences that any increase in the number M of analysis windows allows to lower the standard deviation. Moreover, (8) shows that the longer the sequence is, the higher the average fluctuations amplitude is. Thus, the fluctuations curve highlights high equispaced peaks whose average spacing corresponds to the estimated period symbol T_{s_i}. Therefore, standards can be differentiated like in [7]. It ensures that, the blind synchronization process recently proposed in [8], [9], through which the number N_u^i of active users is determinate, can be performed.

In addition, let us denote ρ, the SNR at the detector input (denoted SNR_{in} (in dB)) of a given signal such that $\sigma^2_{s_{0,0}} = \rho\sigma^2_b$. The ratio (8) to (5) (b), noted $\Gamma_{i,b}$, represents the SNR at the detector output (noted $\text{SNR}_{out}^{(i,b)}$) as explained in [10]

$$\Gamma_{i,b} = \sqrt{\frac{M}{2}} N_u^i L_i T_c W \rho^2. \tag{12}$$

Hence, (12) proves that increasing the number M of windows improves the detection, but at the cost of a larger computing time.

4. Performances analysis

To determine whether a spread spectrum signal is hidden in the noise, a detection threshold η is taken from (5) as

$$\eta = m_{\Phi_b} + \alpha \cdot \sigma_{\Phi_b}, \tag{13}$$

where $\alpha \in \mathbb{N}^*$. Like in the case of radar detection, if this threshold is low, then more targets will be detected at the expense of increased numbers of false alarms. Conversely, if the threshold is high, then fewer targets will be detected, but the number of false alarms will also be low. In most radar detectors, the threshold is set in order to achieve a certain level of false alarm.

4.1. Study within the group *i*, only considering the AWGN

The number M of independent randomly-selected analysis windows is assumed large enough. Hence, for values of τ multiple of T_{s_i}, $\Phi_i(\tau)$ is Gaussian distribution centered in m_{Φ_i} and of variance $\sigma^2_{\Phi_i}$. Then, its probability density $p(\Phi_i)$ is given by:

$$p(\Phi_i) = \frac{1}{\sigma_{\Phi_i}\sqrt{2\pi}} \exp\left\{ -\frac{1}{2}\left(\frac{\Phi_i - m_{\Phi_i}}{\sigma_{\Phi_i}} \right)^2 \right\}. \tag{14}$$

4.1.1. Probability of detection

Let us set as $\mathcal{P}_D^i$ the probability of detecting fluctuations peaks due to signals which belong to the group i, i.e., the probability for the fluctuations average amplitude to be above the threshold η for a given τ multiple of T_{s_i}. From (13), we get

$$\mathcal{P}_D^i = p(\Phi > \eta) = \int_{\eta}^{+\infty} p(\Phi) d\Phi. \tag{15}$$

Equation (15) can be rewritten using the complementary error function *erfc* as

$$\mathcal{P}_D^i = \frac{1}{2} erfc\left(\frac{\eta - m_{\Phi_i}}{\sigma_{\Phi_i}\sqrt{2}} \right). \tag{16}$$

Then, introducing (8), (11) and (13) in (16) leads to

$$\mathcal{P}_D^i = \frac{1}{2} erfc\left\{ \frac{\sqrt{M}}{2} \left(\frac{\left(1 + \alpha\sqrt{\frac{2}{M}}\right)}{N_u^i L_i T_c W \rho^2} - 1 \right) \right\} \tag{17}$$

At this point, let us set as $K = dim(\Phi)$, the number of points of the global fluctuations $\Phi(\tau)$, N_{peak} the minimum number of fluctuations peaks due to signals transmitting at $\min_{i=0,\cdots,S-1}(R_i)$ (hence, spread with the sequence's length $\max_{i=0,\cdots,S-1}(L_i)$) wished to be observed, which depends on M, T_F and F_e, the sampling frequency. It is also useful and important to recall that the detector is designed to work in an interactive way with an operator. Hence, he must choose a sufficient value of K in order to observe, in the case of a good detection, at least 3 or 4 fluctuations peaks due to signals transmitting at the lowest R_i, thus spread with the largest factor L_i.

Moreover, since symbols are assumed independent, the events occurrence of a fluctuations peak for a given value τ multiple of T_{s_i}, can also be considered as independent. Consequently, the global probability of detection, set as $P_{\mathcal{D}}^i$, must take into account the number N_{peak} of fluctuations peaks. Therefore, from (17), we get

$$P_{\mathcal{D}}^i = \left\{ \frac{1}{2} erfc\left\{ \frac{\sqrt{M}}{2} \left(\frac{\left(1 + \alpha\sqrt{\frac{2}{M}}\right)}{N_u^i L_i T_c W \rho^2} - 1 \right) \right\} \right\}^{N_{peak}}. \tag{18}$$

4.1.2. Probability of false alarm

When only focusing on a fluctuations point, its probability, denoted $P_b^{(1)}$ to be above the threshold is

$$P_b^{(1)} = \frac{1}{2} erfc\left(\frac{\eta - m_{\Phi_b}}{\sigma_{\Phi_b}\sqrt{2}} \right) = \frac{1}{2} erfc\left(\frac{\alpha}{\sqrt{2}} \right). \tag{19}$$

Since the false alarms occur when the noise fluctuations are above the threshold at any point τ, the false alarm probability, denoted P_{fa} is defined as

$$1 - P_{fa} = \left(1 - P_b^{(1)}\right)^K, \tag{20}$$

where K allows to take into account all points of the global fluctuations. Then, (20) can be simplified as follows

$$P_{fa} = 1 - \left(1 - \frac{1}{2} erfc\left(\frac{\alpha}{\sqrt{2}} \right)\right)^K. \tag{21}$$

4.2. Extension to the multirate multiuser case

When only two groups i and j of signals ($s_{n,i}$ and $s_{n,j}$) interfere, it is improbable, even impossible, that there are fluctuations peaks due to $s_{n,i}$ where one awaited fluctuations peaks due to $s_{n,j}$, since symbol periods are different. However, if that occurred, that should reinforce the probability to detect the fluctuations peaks due to $s_{n,j}$.

4.2.1. Probability of detection

When there are several groups of signals transmitting at different rates, for given i, the probability $P_{\mathcal{D}/\mathcal{B}}^i$ of detecting the fluctuations peaks due to signals within the group i depends on fluctuations, set as $\Phi_{\mathcal{B}}$, due to both AWGN and MAI noise.

Since symbol periods are different, fluctuations $\Phi_{\mathcal{B}}$ have to be considered at the places where they are not supposed to exhibit peaks, because there, they can be awkward and have a similar effect with that of the noise. Hence, they can be characterized by their mean $m_{\Phi_{\mathcal{B}}}$ as

$$\begin{aligned} m_{\Phi_{\mathcal{B}}} &= \frac{\left(\sigma_b^2 + N_u^i\left(\beta - 1\right)\sigma_{s_{0,0}}^2\right)^2}{WT_F} \\ &= \frac{\sigma_{s_{0,0}}^4\left(1 + N_u^i\left(\beta - 1\right)\rho\right)^2}{WT_F\rho^2}, \end{aligned} \tag{22}$$

where $\beta = \frac{N_u}{N_u^i}$ is the ratio between the total amount of users transmitting at all rates and those transmitting at particular rate R^i, and $N_u\left(\beta - 1\right)\sigma_{s_{0,0}}^2$ is the power of signals inside other groups. Their standard deviation $\sigma_{\Phi_{\mathcal{B}}}$ can be expressed as

$$\sigma_{\Phi_{\mathcal{B}}} = \sqrt{\frac{2}{M}} \frac{\left(\sigma_b^2 + N_u^i(\beta-1)\sigma_{s_{0,0}}^2\right)^2}{WT_F} = \sqrt{\frac{2}{M}} \frac{\sigma_{s_{0,0}}^4 \left(1 + N_u^i(\beta-1)\rho\right)^2}{WT_F\rho^2}. \tag{23}$$

Then, like in (13) a new detection threshold η', taking into account (22) and (23) is defined as

$$\eta' = m_{\Phi_{\mathcal{B}}} + \alpha \cdot \sigma_{\Phi_{\mathcal{B}}}. \tag{24}$$

Since signals are assumed to be received with the same power, using (5) and (24) for any τ neither multiple of T_{s_i} nor multiple of T_{s_j}, $j \neq i$, $j = 0, \cdots, S-1$, we get the expression of η':

$$\eta' = \frac{\sigma_{s_{0,0}}^4}{WT_F} \left\{ \frac{\left(1 + N_u^i(\beta-1)\rho\right)^2}{\rho^2} \left(1 + \alpha\sqrt{\frac{2}{M}}\right) \right\}. \tag{25}$$

Hence, focusing on a peak, the probability $\mathcal{P}_{\mathcal{D}/\mathcal{B}}^i$ of detecting fluctuations due to signals in the group i is

$$\mathcal{P}_{\mathcal{D}/\mathcal{B}}^i = \frac{1}{2} erfc\left(\frac{\eta' - m_{\Phi_i}}{\sigma_{\Phi_i}\sqrt{2}} \right), \tag{26}$$

which can be expressed using (8), (11) and (25) as

$$\mathcal{P}_{\mathcal{D}/\mathcal{B}}^i = \frac{1}{2} erfc\left\{ \frac{\sqrt{M}}{2} \left\{ \frac{\left(1 + N_u^i(\beta-1)\rho\right)^2 \left(1 + \alpha\sqrt{\frac{2}{M}}\right)}{N_u^i L_i T_c W \rho^2} - 1 \right\} \right\}. \tag{27}$$

Finally, like in (18), the global probability of detection, set as $P_{\mathcal{D}/\mathcal{B}}^i$, taking into account the number N_{peak} of fluctuations peaks is given by

$$P_{\mathcal{D}/\mathcal{B}}^i = \left(\mathcal{P}_{\mathcal{D}/\mathcal{B}}^i\right)^{N_{peak}}. \tag{28}$$

4.2.2. Probability of false alarm

If we first focus on a fluctuations peak of signals within the group i, and since the false alarm is due to the fluctuations of the global noise (additive noise and MAI noise), its probability, noted $P_{\mathcal{B}}^{(1)}$, to be above the threshold is

$$P_{\mathcal{B}}^{(1)} = \frac{1}{2} erfc\left(\frac{\eta' - m_{\Phi_{\mathcal{B}}}}{\sigma_{\Phi_{\mathcal{B}}}\sqrt{2}} \right) = \frac{1}{2} erfc\left(\frac{\alpha}{\sqrt{2}} \right). \tag{29}$$

Thus, as previously detailed in the multiuser single rate case, the probability of false alarm is the same as in (21). Finally, like in (12), let us set as $\Gamma_{i,B}$ the ratio (8) to (23) (noted

$SNR_{out}^{(i,B)}$), which stands for the SNR at the detector output

$$\Gamma_{i,B} = \sqrt{\frac{M}{2}} \frac{N_u^i L_i T_c W \rho^2}{\left(1 + N_u^i \left(\beta - 1\right) \rho\right)^2}. \tag{30}$$

4.3. Remarks and analysis

$\Gamma_{i,b}$ and $\Gamma_{i,B}$ are close for low SNRs or when the total number N_u of users is equal to N_u^i. However, for high SNRs, $\Gamma_{i,b}$ increases with ρ^2, while $\Gamma_{i,\mathcal{B}}$ is bounded as

$$\Gamma_{i,\mathcal{B}} \leq \max(\Gamma_{i,\mathcal{B}}) = \sqrt{\frac{M}{2}} \frac{N_u^i L_i T_c W}{\left(N_u^i \left(\beta - 1\right)\right)^2}. \tag{31}$$

Moreover, for high SNRs, the ratio (30) to (12) leads to (in dB)

$$SNR_{out}^{(i,B)} = SNR_{out}^{(i,b)} - 20\log\left(1 + N_u^i \left(\beta - 1\right) \rho\right). \tag{32}$$

Equation (32) shows a loss of $20\log\left(1 + N_u^i \left(\beta - 1\right) \rho\right)$ dB at the detector output in the multiuser multirate case compared to the single rate one. However, the same performances can be achieved by increasing for example M as also proved in (31), but at the expense of a higher computation time.

Let us set as $\Delta_{(m_{\Phi_i},\eta)}$ the ratio (8) to (13), and $\Delta'_{(m_{\Phi_i},\eta')}$ the ratio (8) to (25). Then, we get

$$\Delta_{(m_{\Phi_i},\eta)} = \frac{N_u^i L_i T_c W \rho^2}{1 + \alpha\sqrt{\frac{2}{M}}}, \tag{33}$$

$$\Delta'_{(m_{\Phi_i},\eta')} = \frac{N_u^i L_i T_c W \rho^2}{\left(1 + N_u^i (\beta - 1)\rho\right)^2 \left(1 + \alpha\sqrt{\frac{2}{M}}\right)}. \tag{34}$$

In addition, if the number of analysis windows M is chosen large enough, i.e., $M \gg 2\alpha^2$, (33) and (34) can be rewritten as

$$\widetilde{\Delta}_{(m_{\Phi_i},\eta)} = N_u^i L_i T_c W \rho^2, \tag{35}$$

$$\widetilde{\Delta}'_{(m_{\Phi_i},\eta')} = \frac{N_u^i L_i T_c W \rho^2}{\left(1 + N_u^i (\beta - 1)\rho\right)^2}. \tag{36}$$

Moreover, in the case $M \gg 2\alpha^2$, (17) can be approximated by

$$\tilde{\eta}' = \frac{\sigma_{s_{0,0}}^4}{W T_F} \left\{ \frac{\left(1 + N_u^i \left(\beta - 1\right) \rho\right)^2}{\rho^2} \right\}. \tag{37}$$

Then, the following equations give the approximations of probabilities of detection (18) and (28).

$$\widetilde{P}_{\mathcal{D}}^{i}=\left\{\frac{1}{2}erfc\left\{\frac{\sqrt{M}}{2}\left(\frac{1}{N_u^i L_i T_c W \rho^2}-1\right)\right\}\right\}^{N_{peak}}, \tag{38}$$

$$\widetilde{P}_{\mathcal{D}/\mathcal{B}}^{i}=\left\{\frac{1}{2}erfc\left\{\frac{\sqrt{M}}{2}\left\{\frac{\left(1+N_u^i\left(\beta-1\right)\rho\right)^2}{N_u^i L_i T_c W \rho^2}-1\right\}\right\}\right\}^{N_{peak}}. \tag{39}$$

It is obvious to check that (36) and (39) are equivalent to (35) and (38) respectively, by setting $\beta=1$, which corresponds to the case $N_u=N_u^i$, i.e., when all users are transmitting at one rate R_i.

Moreover, (38) and (39) exhibit a similar behavior asymptotically. Thus, whatever the MAI noise power is, the probability of detection can be improved just by increasing the number of windows M. However, it depends on both the available computation power and the time allocated for the detection.

5. Numerical results

5.1. Detector's parameters setting

Let us set as T_s the duration of the global intercepted signal, $F_c=\frac{1}{T_c}$, the common chip frequency, $F_e=\frac{1}{T_e}$, the sampling frequency at the detector input. It ensues that the total number N_e of samples of the signal to analyze and the number M of analysis windows can be expressed as

$$\begin{cases} N_e = 2^{\left\lfloor \ln\left(\frac{T_S}{T_e}\right)\right\rfloor} \\ M=\dfrac{T_S}{T_e} \end{cases} \tag{40}$$

where $\lfloor * \rfloor$ stands for the integer part of $*$. Let us also recall that the average spacing between fluctuations peaks gives an estimate of symbol periods inside each group i. Consequently, since the detector is designed to work in an interactive way with an operator, some parameters can be set according to the number of peaks which one wishes to observe. Without detailing calculations, following equations give K and N_{peak}^i.

$$K=\left\lfloor \frac{\gamma F_e L_i^{max}}{F_c} \right\rfloor, \tag{41}$$

$$N_{peak}^i=\gamma\frac{L_i^{max}}{L_i}, \quad L_i \neq L_i^{max}. \tag{42}$$

where $L_i^{max}=\max_{i=0,\cdots,S-1}(L_i)$, γ is a real coefficient to be adjusted in order to obtain the minimum number of peaks wished for users whose signals are spread with the processing gain L_i^{max}, and N_{peak}^i stands for the minimum number of fluctuations peaks within each group i.

Moreover, since the signal spectrum must be contained in the detector's ADC (Analog to Digital Converter) bandwidth, W has to satisfy $F_c \le W \le F_e$. A last, for signals transmitting at R_i, the number of symbols N_{s_i} contained within an analysis window is given by

$$N_{s_i} = \left\lfloor \frac{T_F}{L_i T_c} \right\rfloor. \tag{43}$$

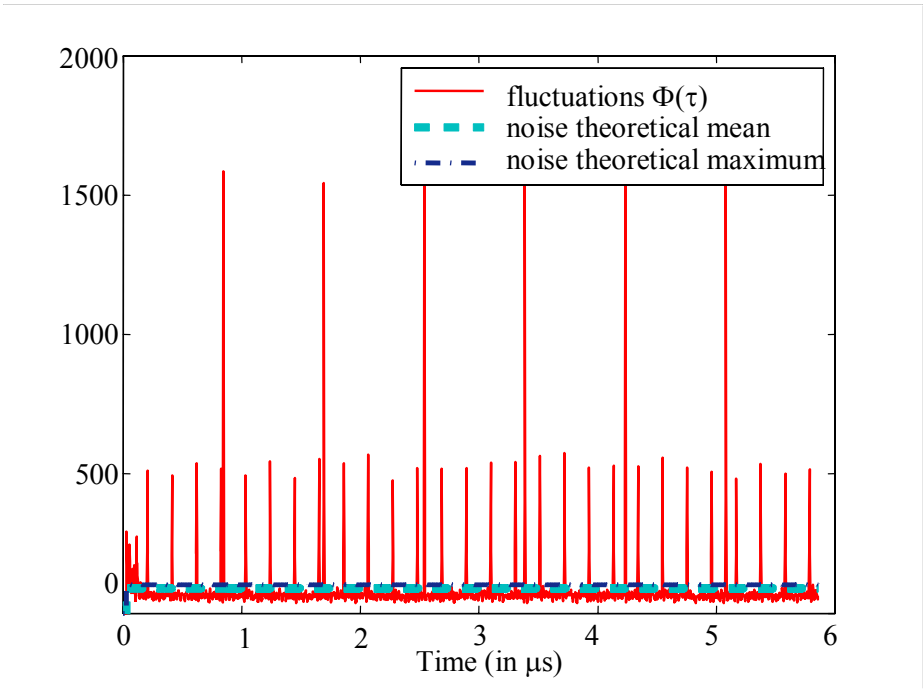

Figure 1. Fluctuations $\Phi(\tau), N_u^0 = 2, N_u^1 = 2, SNR_{in} = -5$ dB.

Figure 1 was obtained with processing gains of $L_0 = 31$, $L_1 = 127$ (complex Gold sequences), and $\alpha = 3$. It also was set $F_c = \frac{1}{T_c} = 150\ MHz$, the common chip frequency, $W = 200\ MHz$, the analysis bandwidth, $F_e = 300\ MHz$, the sampling frequency, $T_F = 2\ \mu s$, $M = 375$, $N_u^0 = 2$ and $N_u^1 = 2$, hence $N_u = 4$. The global intercepted signal is of duration $T_s = 750\ \mu s$ and belong to QPSK constellation. Hence, the intercepted signal corresponds to $N_e = 131072$ samples. For $\gamma = 3.5$, $K = 889$, $N_{peak} = 6$, and each analysis window contains about 10 symbols for users transmitting at R_0 and 3 for users transmitting at R_1.

The curve shows the fluctuations of the autocorrelation estimator $\Phi(\tau)$. It clearly highlights two sets of equispaced peaks of different amplitudes. It means that two sets of spread spectrum signals transmitting at two different rates are hidden in the noise. Then, as detailed in [5], we find (in μs) $T_{s_0} = 0.2061$ and $T_{s_1} = 0.8467$.

5.2. Performances analysis

Figure 2 illustrates the probability of false alarm P_{fa} according to the number K of analysis points for different values of α. It evidences that any increase in the threshold concomitantly with K induces a decrease of P_{fa}. However, that also lowers the probability of

detection. Thus, $\alpha = 3$ and $K = 889$ seem to be a good trade-off between P_{fa} and the probability of detection.

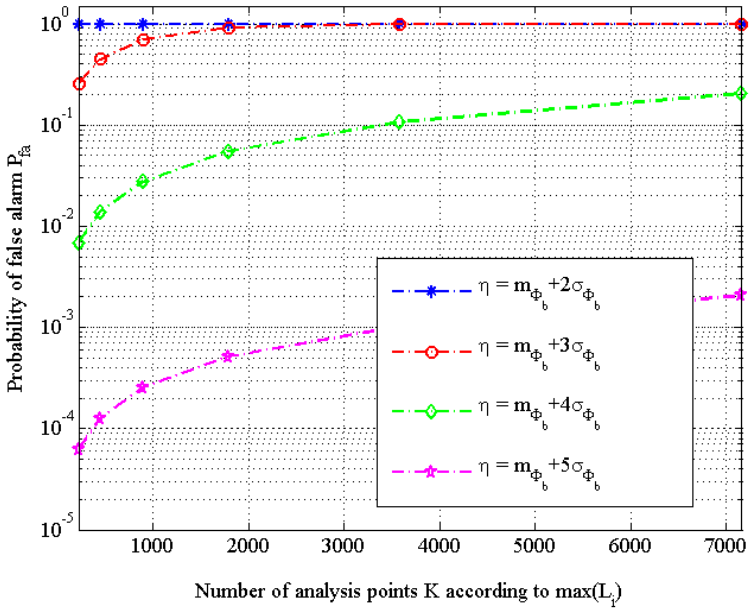

Figure 2. Probability of false alarm according to K for different thresholds.

Figure 3 and Figure 4 show the ratio (8) to (13) in dB, set as $\Delta_{(m_{\Phi_i},\eta)}$ in the multiuser single rate case. As it can be seen, $\Delta_{(m_{\Phi_i},\eta)}$ is above 0 dB, which allows the blind detection, except for $SNR_{in} = -40$ dB. However, $\Delta_{(m_{\Phi_i},\eta)}$ can be improved just by increasing the number M of analysis windows. In addition, Figure 4 shows that with the same threshold, $\Delta_{(m_{\Phi_i},\eta)}$ will be higher than 0 dB for largest sequence lengths. Hence, any increase in the threshold involves a degradation of the ratio $\Delta_{(m_{\Phi_i},\eta)}$, except for largest sequence lengths.

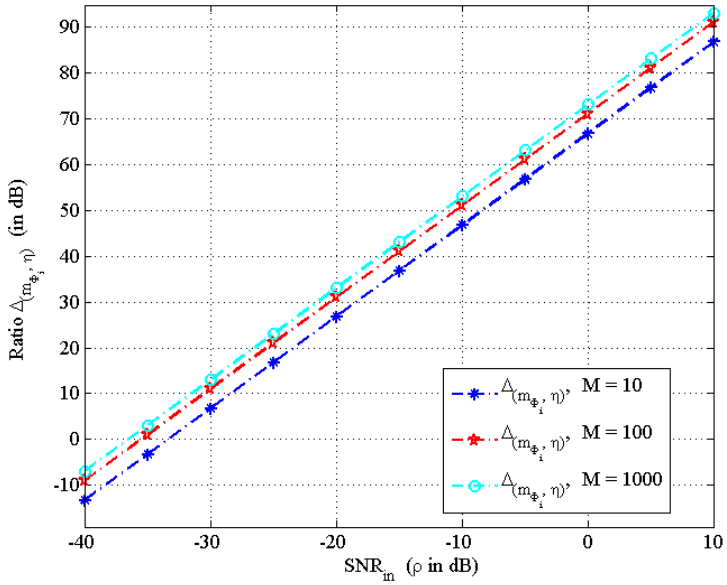

Figure 3. $\Delta_{(m_{\Phi_i},\eta)}$, $\alpha = 3$, $N_u^i = 30$, $L_i = 127$, $W = 200$ MHz, $T_c = 150$ MHz, $F_e = 300$ MHz.

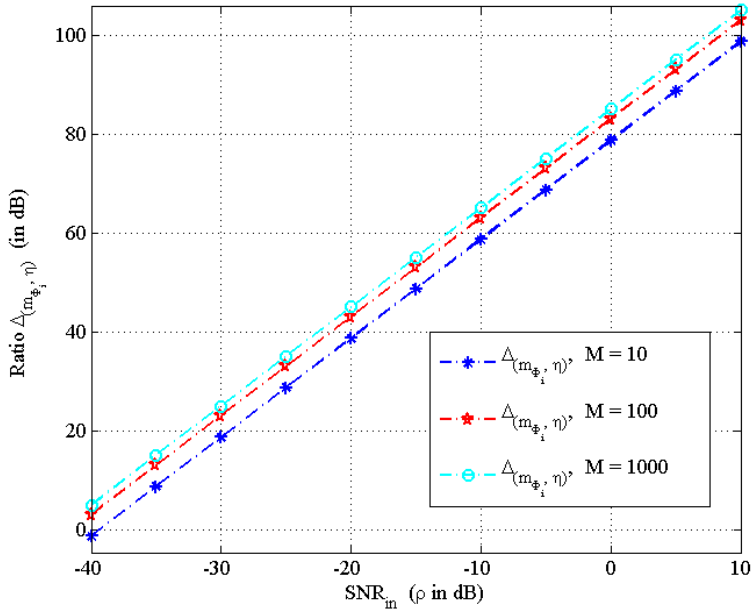

Figure 4. $\Delta_{(m_{\Phi_i},\eta)}$, $\alpha = 3$, $N_u^i = 30$, $L_i = 511$, $W = 200\,\text{MHz}$, $T_c = 150\,\text{MHz}$, $F_e = 300\,\text{MHz}$.

Figure 5 and Figure 6 show the ratio (8) to (25), set as $\Delta'_{(m_{\Phi_i},\eta')}$ in the multiuser multirate case, for different SNR_{in} and β. It is clearly shown that any increase in β induces a decrease of the ratio $\Delta'_{(m_{\Phi_i},\eta')}$. Nevertheless, this ratio can be improved by adjusting the number M of analysis windows. In agreement with previous figures, the larger the sequence length is the highest $\Delta'_{(m_{\Phi_i},\eta')}$ is, which increases the probability of detection.

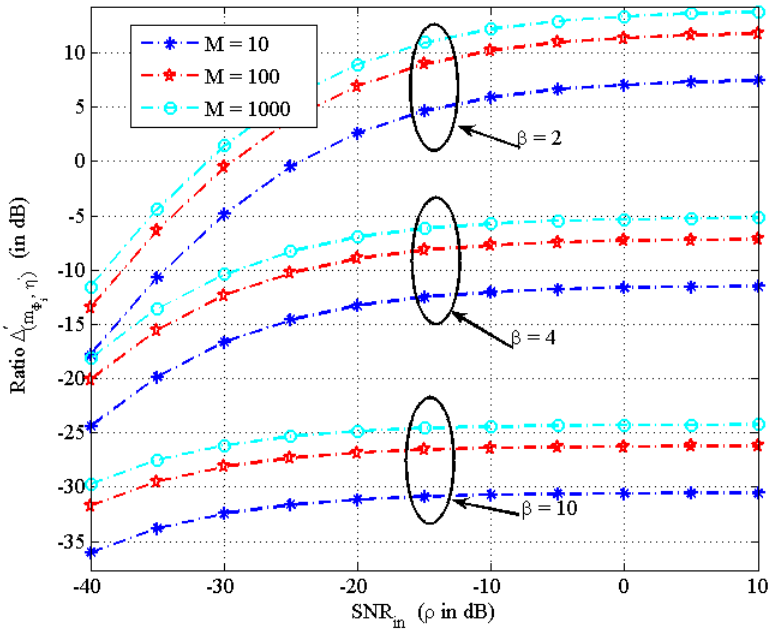

Figure 5. $\Delta'_{(m_{\Phi_i},\eta')}$, $\alpha = 3$, $N_u^i = 30$, $L_i = 127$, $W = 200\,\text{MHz}$, $T_c = 150\,\text{MHz}$, $F_e = 300\,\text{MHz}$.

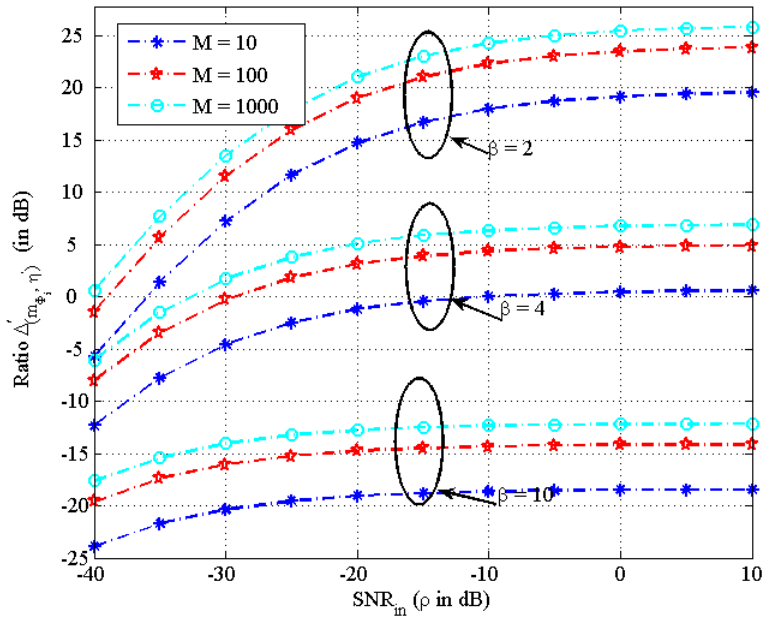

Figure 6. $\Delta'_{(m_{\Phi_i},\eta')}$, $\alpha = 3$, $N_u^i = 30$, $L_i = 511$, $W = 200\,\text{MHz}$, $T_c = 150\,\text{MHz}$, $F_e = 300\,\text{MHz}$.

In addition, it is obvious that when the threshold increases, best performances are achieved with the largest sequence lengths as highlighted on Figure 7 and Figure 8.

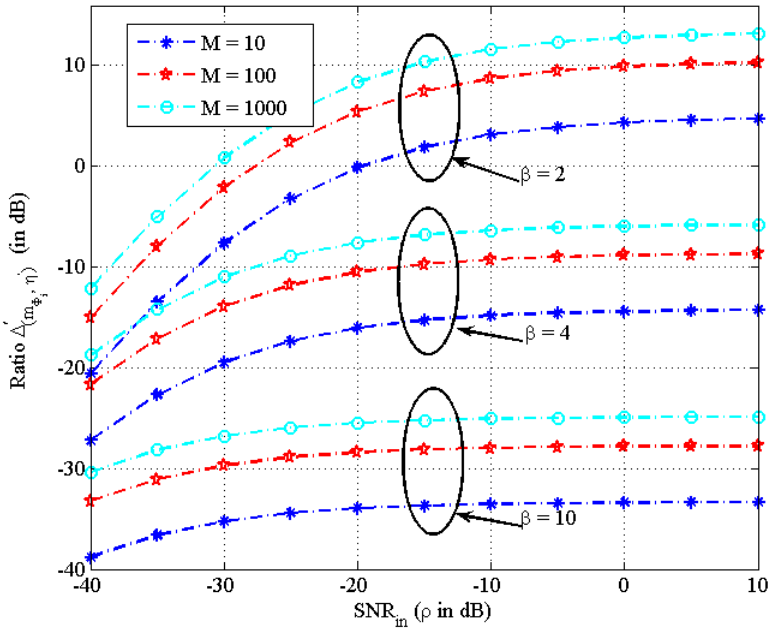

Figure 7. $\Delta'_{(m_{\Phi_i},\eta')}$, $\alpha = 5$, $N_u^i = 30$, $L_i = 127$, $W = 200\,\text{MHz}$, $T_c = 150\,\text{MHz}$, $F_e = 300\,\text{MHz}$.

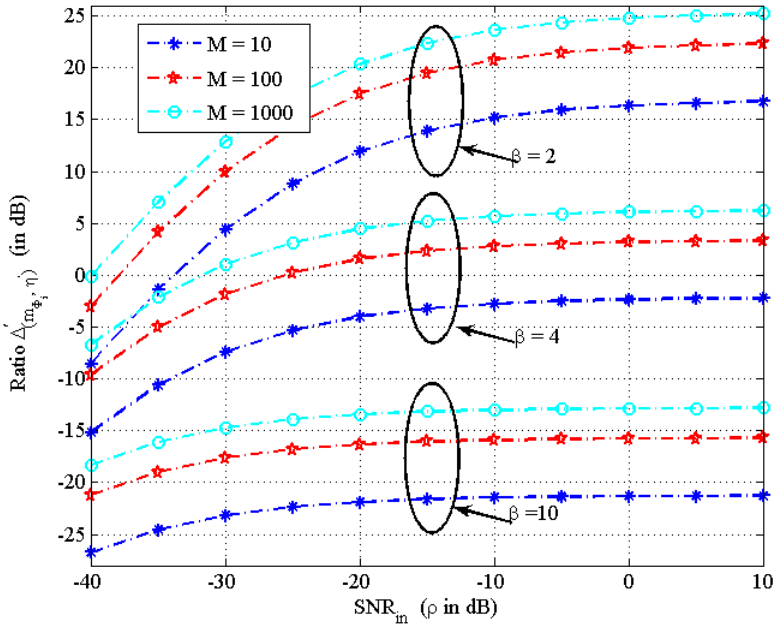

Figure 8. $\Delta'_{(m_{\Phi_i},\eta')}$, $\alpha = 5$, $N_u^i = 30$, $L_i = 511$, $W = 200\,\text{MHz}$, $T_c = 150\,\text{MHz}$, $F_e = 300\,\text{MHz}$.

Figure 9 and Figure 10 illustrate the probability of detection $P_{\mathcal{D}}^i$ in the multiuser single rate case. They evidence that any increase in the number M of analysis windows induces an increase of $P_{\mathcal{D}}^i$. Moreover, for larger M, i.e., $M \geq 2\alpha^2$, approximated probabilities curves are very close to the real ones, in agreement with theoretical analysis. In addition, the larger the sequence length is the highest $P_{\mathcal{D}}^i$ is.

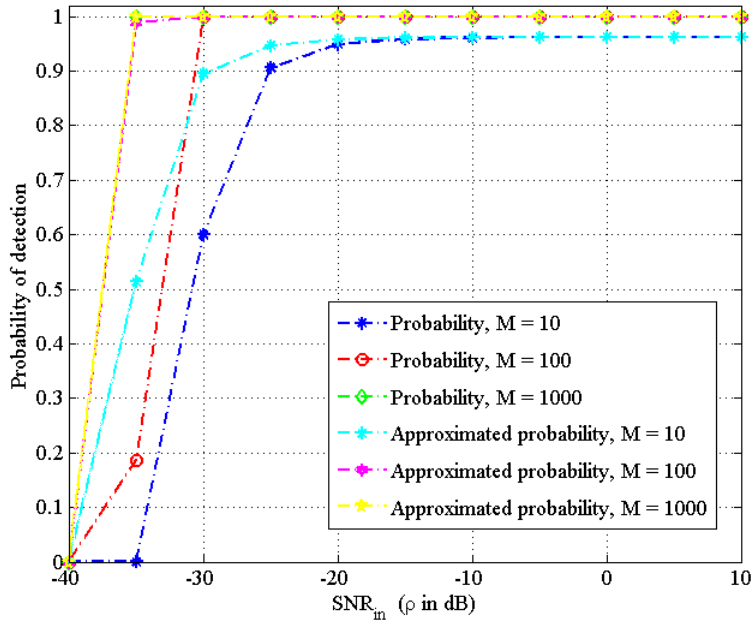

Figure 9. $P_{\mathcal{D}}^i$ according to M and SNR_{in}, $\beta = 2$, $\alpha = 3$, $N_u^i = 30$, $L_i = 127$, $W = 200\,\text{MHz}$, $T_c = 150\,\text{MHz}$, $F_e = 300\,\text{MHz}$.

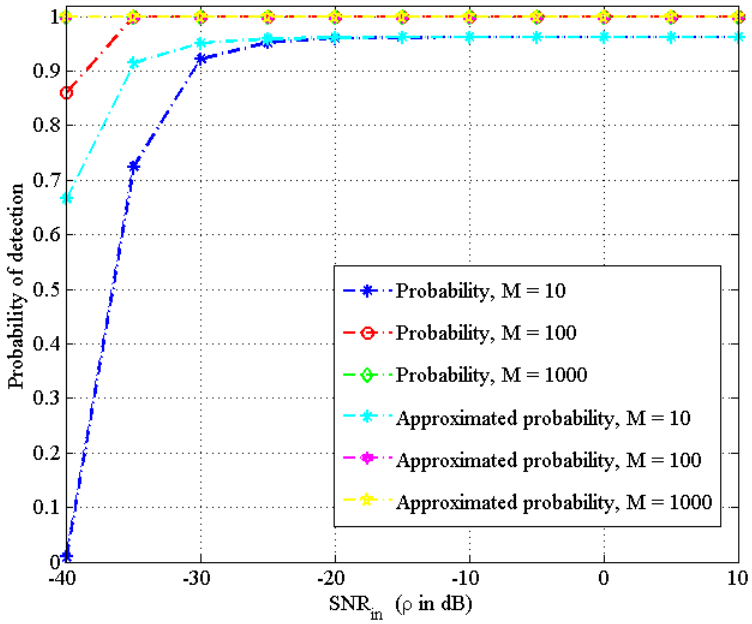

Figure 10. $P_{\mathcal{D}}^{i}$ according to M and SNR_{in}, $\beta = 2$, $\alpha = 3$, $N_u^i = 30$, $L_i = 511$, $W = 200\,\text{MHz}$, $T_c = 150\,\text{MHz}$, $F_e = 300\,\text{MHz}$.

Figure 11 and Figure 12 depict the probability of detection $P_{\mathcal{D}/\mathcal{B}}^{i}$ in the multiuser multirate case. They first show that approximated probabilities curves are very close to the real ones. Second, for a fixed threshold, the probability of detection increases concomitantly with sequence lengths. Moreover, any increase in the number M of analysis windows improves the probability of detection.

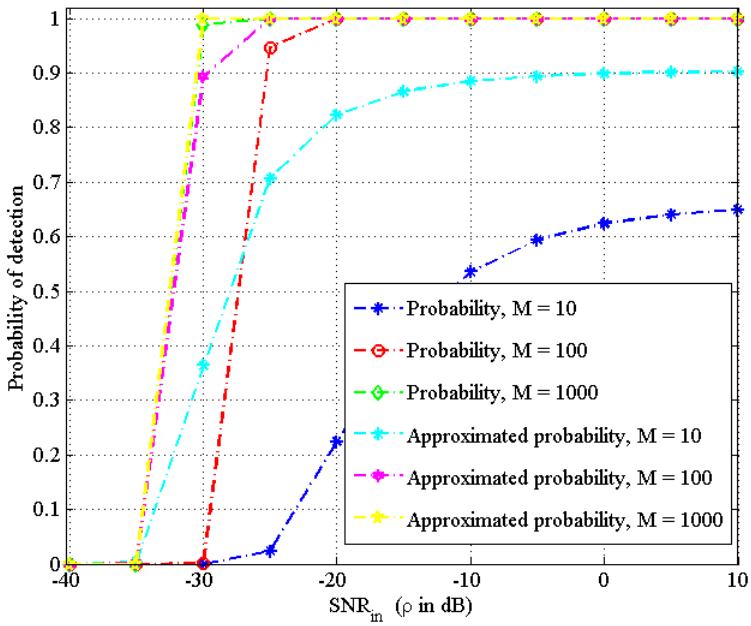

Figure 11. $P_{\mathcal{D}/\mathcal{B}}^{i}$ according to M and SNR_{in}, $\beta = 2$, $\alpha = 3$, $N_u^i = 30$, $L_i = 127$, $W = 200\,\text{MHz}$, $T_c = 150\,\text{MHz}$, $F_e = 300\,\text{MHz}$.

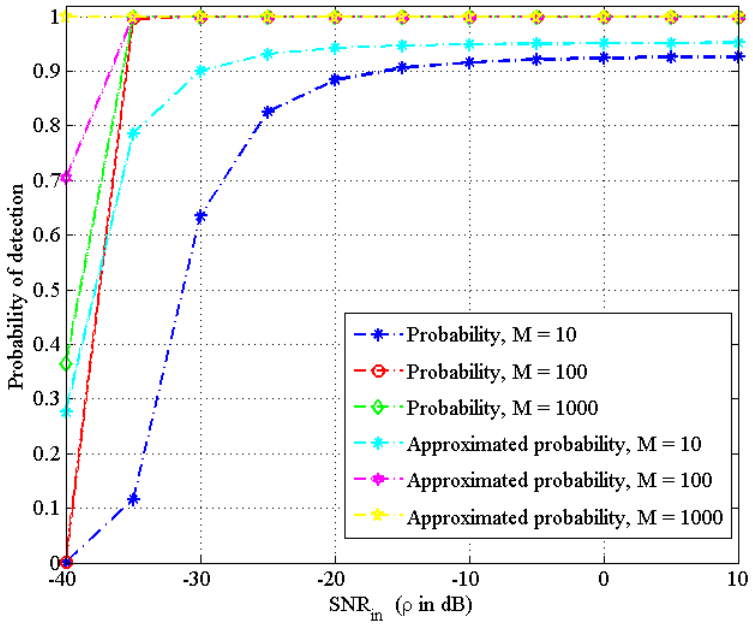

Figure 12. $P^i_{\mathcal{D}/\mathcal{B}}$ according to M and SNR_{in}, $\beta = 2$, $\alpha = 3$, $N^i_u = 30$, $L_i = 511$, $W = 200\,\text{MHz}$, $T_c = 150\,\text{MHz}$, $F_e = 300\,\text{MHz}$.

In addition, for larger thresholds, performances can be improved either by an increase of the number of analysis windows, or by detecting first fluctuations peaks corresponding to largest spreading codes lengths, as shown in Figure 13 and Figure 14. Let us note that one also could adjust the other parameters of the detection, since the detection method described herein this paper can be performed in an interactive way.

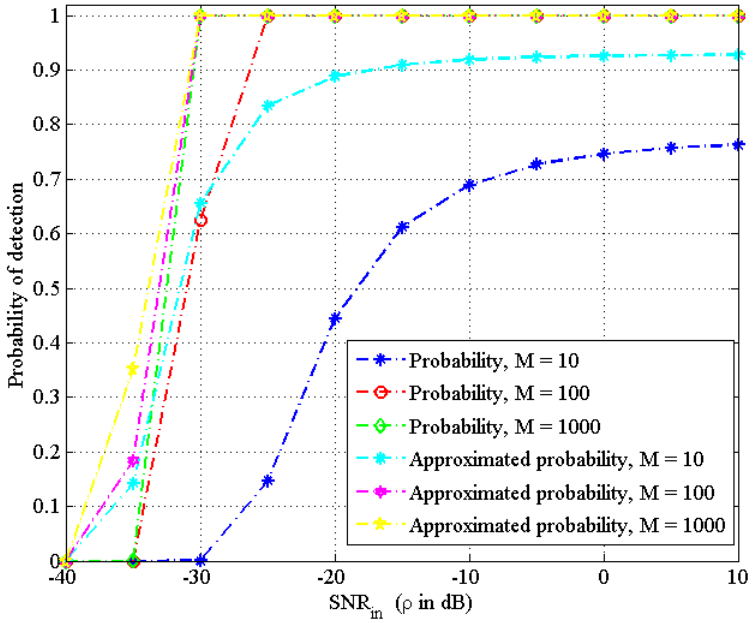

Figure 13. $P^i_{\mathcal{D}/\mathcal{B}}$ according to M and SNR_{in}, $\beta = 2$, $\alpha = 5$, $N^i_u = 30$, $L_i = 127$, $W = 200\,\text{MHz}$, $T_c = 150\,\text{MHz}$, $F_e = 300\,\text{MHz}$.

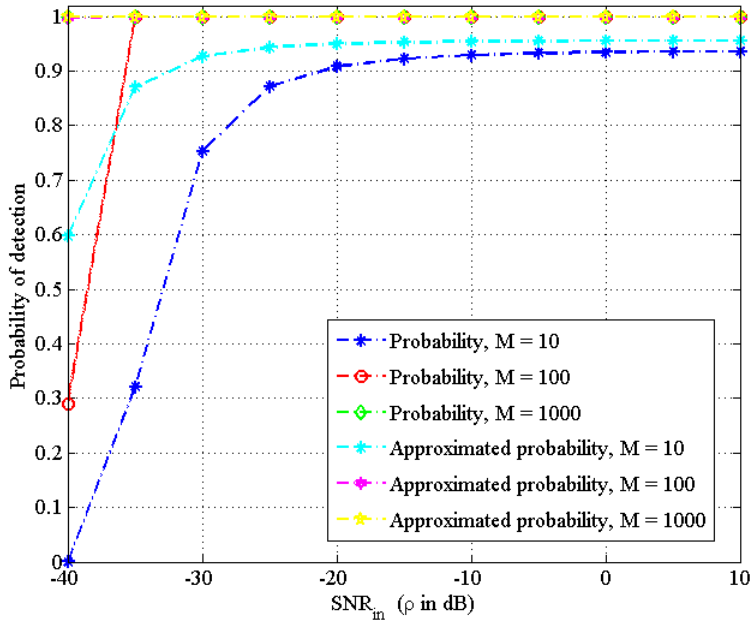

Figure 14. $P_{\mathcal{D}/\mathcal{B}}^{i}$ according to M and SNR_{in}, $\beta = 2$, $\alpha = 5$, $N_u^i = 30$, $L_i = 511$, $W = 200\,\text{MHz}$, $T_c = 150\,\text{MHz}$, $F_e = 300\,\text{MHz}$.

As expected, Figure 15 and Figure 16 highlight a loss of $20\log\left(1+N_u^i\left(\beta-1\right)\rho\right)$ in the $SNR_{out}^{(i,B)}$ (i.e., the SNR at the detector output in the multiuser multirate case) compared to the $SNR_{out}^{(i,b)}$ (i.e., the SNR at the detector output in the multiuser single rate case). However, for low SNRs at the detector input, $SNR_{out}^{(i,B)}$ and $SNR_{out}^{(i,b)}$ are close.

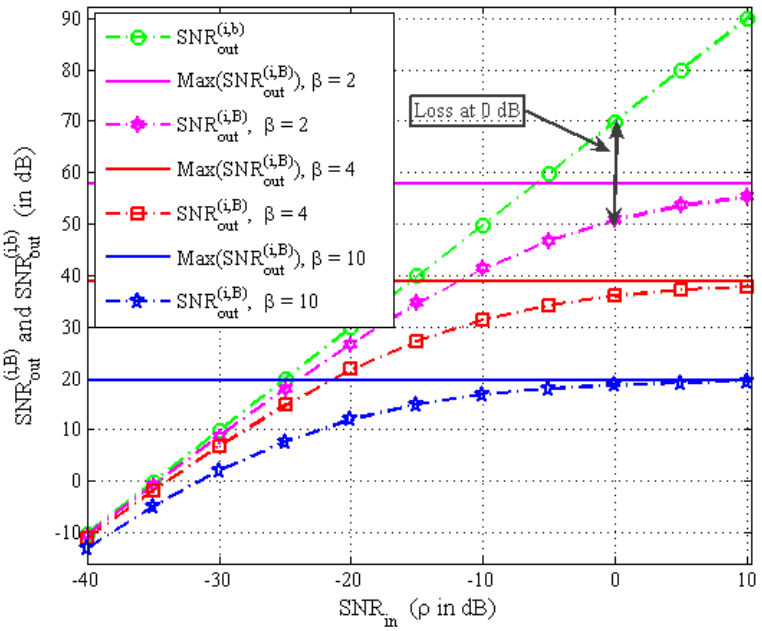

Figure 15. Comparison of $SNR_{out}^{(i,b)}$ and $SNR_{out}^{(i,\mathcal{B})}$ at the detector output for given β, $M = 300$, $N_u^i = 2$, $L_i = 127$, $W = 200\,\text{MHz}$.

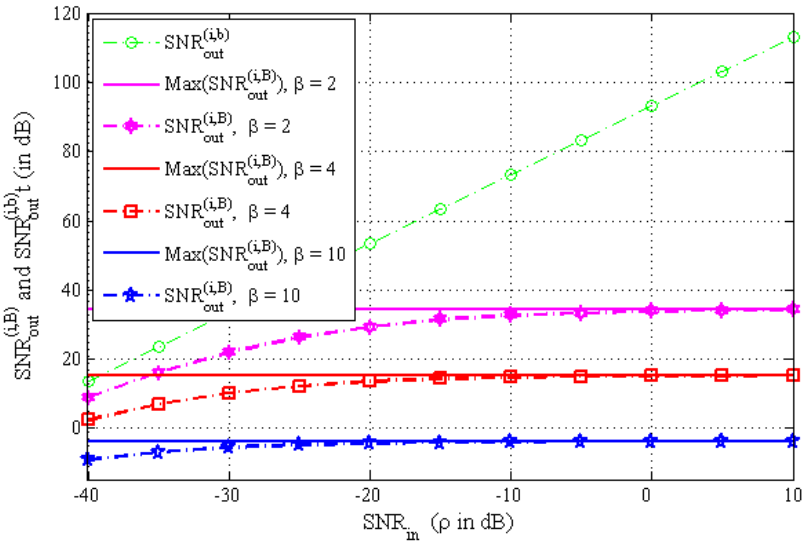

Figure 16. Comparison of $SNR_{out}^{(i,b)}$ and $SNR_{out}^{(i,\mathcal{B})}$ at the detector output for given β, $M = 300$, $N_u^i = 30$, $L_i = 127$, $W = 200\,\text{MHz}$.

They clearly evidenced that any increase in the number N_u^i of users within i, in an equivalent way, any increase in the global number N_u of interfering users, lowers the $SNR_{out}^{(i,B)}$ maximum. Nevertheless, the $SNR_{out}^{(i,B)}$ remains sufficiently high, which proves the efficiency of the proposed blind detection approach.

Moreover, and as discussed herein this paper, the $SNR_{out}^{(i,B)}$ can be significantly improved by increasing the number M of analysis windows or adjusting the other detection parameters.

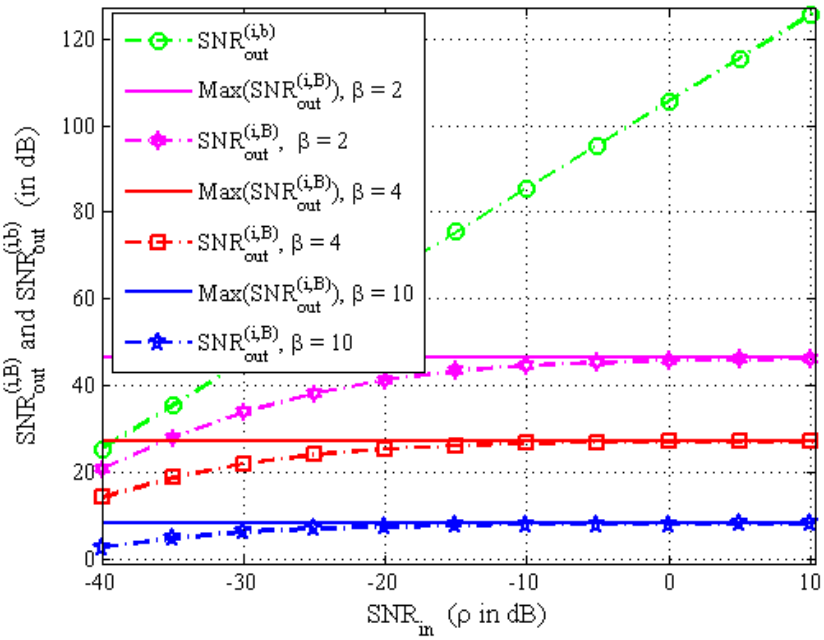

Figure 17. Comparison of $SNR_{out}^{(i,b)}$ and $SNR_{out}^{(i,\mathcal{B})}$ at the detector output for given β, $M = 300$, $N_u^i = 30$, $L_i = 511$, $W = 200\,\text{MHz}$.

At last, Figure 17 that despite the increase in the number of active users, the $SNR_{out}^{(i,B)}$ can be strongly improved by focusing first on fluctuations peaks due to signals spread with the largest sequences lengths.

6. Conclusion

We have evidenced the efficiency of the blind multiuser multirate detection method based on fluctuations of correlation estimators through its theoretical analysis. Assuming a large number of independent randomly-selected analysis windows, we have expressed second-order moments of fluctuations due to both signals and noise. Then, we have derived the probabilities of detection in both multirate and single rate case.

Moreover, the analysis of detection probabilities, confirmed by numerical results have proved that very good performances in terms of probability of detection and false alarm can be achieved, even at very low SNRs or with many interfering users.

At last, we demonstrated that performances could be significantly improved just by increasing the number of analysis windows, but at the expense of a higher computation time.

Acknowledgment

This work was partially supported by the Brittany Region (France).

References

[1] S. Roy, “Subspace blind adaptive detection for multiuser CDMA,” IEEE Transactions on Communications, vol. 48, no. 1, January 2000.

[2] X. Wang and A. Host-Madsen, “Group-blind multiuser detection for uplink CDMA,” IEEE Journal on Selected Areas in Communications, vol. 17, no. 11, pp. 1971-1984, November 1999.

[3] A. Haghighat and M. R. Soleymani, “A subspace scheme for blind user identification in multiuser DS-CDMA,” in IEEE-WCNC, vol. 4, no. 1, pp. 688-692, March 2003.

[4] S. Buzzi, M. Lops, and A. Pauciullo, “Iterative cyclic subspace tracking for blind adaptive multiuser detection in multirate CDMA systems,” IEEE Transactions on Vehicular Technology, vol. 52, no. 6, pp. 1463-1475, November 2003.

[5] C. Nsiala Nzéza, R. Gautier, and G. Burel, “Blind Multiuser Detection in Multirate CDMA Transmissions Using Fluctuations of Correlation Estimators,” in 49th IEEE-GlobeCom Conference, San Francisco, California, USA, November 2006.

[6] Crépin Nsiala Nzéza, “Récepteur adaptatif multi-standards pour les signaux à étalement de spectre en contexte non coopératif,” Ph.D. dissertation, Université de Bretagne Occidentale, Brest, France, July 2006.

[7] C. Williams, M. Beach, D. Neirynck, A. Nix, K. Chen, K. Morris, D. Kitchener, M. Presser, Y. Li, and S. McLaughlin, “Personal area technologies for internetworked services,” IEEE Communications Magazine, vol. 42, no. 12, pp. s15-s32, December 2004.

[8] C. Nsiala Nzéza, R. Gautier, and G. Burel, “Parallel Blind Multiuser Synchronization and Sequences Estimation in Multirate CDMA Transmissions,” in 40th IEEE-Asilomar

Conference on Signals, Systems, and Computers, Pacific Grove, California, USA, pp. 2157-2161, October 2006.

[9] C. Nsiala Nzéza, R. Gautier, and G. Burel, "Blind Multiuser Identification in Multirate CDMA Transmissions : A New Approach," in 40th IEEE-Asilomar Conference on Signals, Systems, and Computers, Pacific Grove, California, USA, pp. 2162-2166, October 2006.

[10] G. Burel, "Detection of spread spectrum transmission using fluctuations of correlation estimators," in IEEE Int. Symp. On Intelligent Signal Processing and Communications Systems (ISPAC'2000), Honolulu, Hawaii, USA, November 5-8, 2000.